Russian Academy of Sciences
Karelian Scientific Centre
Northern Water Problems Institute

Proceedings of the 7th Workshop on

PHYSICAL PROCESSES IN NATURAL WATERS

2-5 July 2003
Petrozavodsk, Russia

Petrozavodsk, 2003

Study of physical processes in coastal zone for detecting anthropogenic impact by means of remote sensing

Valery G. Bondur[1] and Nikolai N. Filatov[2]

[1] Scientific-educational center "Aerokosmos" of Moscow State University of Geodesy and Cartography, Moscow, E-mail: vgbondur@online.ru
[2]Northern Water Problems Institute, Petrozavodsk, Russia;
E-mail: nfilatov@nwpi.karelia.ru

A complex study of physical processes in the coastal zone for detecting anthropogenic impact on coastal waters by means of remote sensing was performed in the shelf zone of Oahu Island, Hawaii in August-September 2002 (Bondur, Vinogradov et al, 2003). Using observational data from the buoy stations, analysis of surface and internal waves, turbulence, microstructure, currents and tides was done.

Materials and methods of investigations

Several buoy stations were installed for registrations, i.e. two buoy stations on the shelf zone on depths ~60 m for measuring currents with use of ADCP, one buoy station with Aanderaa thermistor chain, three buoy stations to measure surface waves (Sullivan, Dayananda, 1996; Oceanit, 2003). Also, measurements of turbulence, microstructure, temperature fields, salinity and conductivity using sondes (MSS) were performed from the boat board (Gibson et al, 2003). A methodology for detecting submerged outfall, wastewaters and to determine their shape and size with use of high-resolution remote sensing data from satellites Ikonos-2 and QuickBird was developed.

Currents

A variability of currents was analyzed in the time scales varying from several minutes up to 36 hours, i.e. from the Vaisial-Brendt's frequency to the local inertial period. 3D progressive vector diagrams of currents observed at the stations B2 and B4 for various depths were calculated. These diagrams enabled to determine trajectories of water masses. An along-shore flow having direction of 220^o (i.e. SW) is dominant at the depths of 10, 30 and 60 m with quasi-wave fluctuations of current fields in the southwest – southeast directions.

At the station located in the proximity of the diffuser, the components V_e and V_n at all the depths are mainly affected by semidiurnal tidal oscillations. It should be also pointed out that the oscillations of amplitudes of velocities at all the levels are practically synchronous.

Vector-Algebraic Method for Analyzing ocean currents

The data on velocities of currents collected in September 2002 within the framework of the project was processed with use of analysis of vector time series. At present, due to lack of uniform generally accepted technique of analysis of time series, data processing for currents is performed on the basis of substitution of velocity vector: projections of velocity vector to Cartesian axis (component method); complex-valued method that represents complex number, its real and imaginary members being equal to the projections of velocity vector to Cartesian axis; method of rotary-components (see Mooers, 1973; Gonella, 1972). In this work, the advanced vectorial-algebraic method developed by Rozhkov et al. (1983) was applied. The most general model of the ocean currents is their representation in a form of non-stationary non-homogeneous vectorial stochastic functions with values in Euclidean space (see Limnology and Remote sensing, 1999).

As the main probability characteristics of current velocities we assume expectation vector V, correlation tensor determined as an expectation of tensor product of vectors and also spectral

density tensors determined through one- and two-fold Fourier's transformation of the correlation function. Functions *Sv* (•) characterize distribution by the frequencies of oscillations of current velocities and give a quantitative measure of intensity of such oscillations and their orientation in the accepted system of coordinates and changes in time. The abovementioned probability characteristics are invariant by the method of determination, and do not depend on the choice of a system of coordinates. The properties of the tenser-functions *Kv (•),* and so the process *V*(t) properties may be most completely opened through the set of invariant scalar functions; characterize by correspondingly interrelation of collinear and orthogonal components (or their Fourier's function) of the vectorial process. Central problems of processing and analysis of natural data are formulation of the estimation rule and determination of the measure of proximity of estimate to the probability characteristic.

Time series analysis of vector currents in the experiment allows us establishing the dominance of tidal semidiurnal phenomena (ω~0.5 rad·h^{-1}), there were also detected small diurnal (ω~0.26 rad·h^{-1}), long-period (ω<0.1 rad·h^{-1}) and 6 hour (ω~1 rad·h^{-1}) fluctuations. Diurnal fluctuations of currents in upper layers (0-10 m) are caused by diurnal variations of meteorological parameters. Analysis of high-frequency spectral bands of horizontal and vertical components of current vector has shown that the short-period internal waves also have turbulent motions of diverse genesis. The tidal ellipse at the upper level has a greater anisotropy compared to that observed at the depth more than 30 m. In relatively high-frequency spectral band of currents ($\omega \geq 1.0$ rad·h^{-1}) any noticeable fluctuations of velocities were not observed. Thus, as our analysis of the rotation indicator shows, in low-frequency range the rotation was clockwise (inertial oscillations) while the tidal component rotating counter-clockwise at all depths. The rotation of vector of currents with semidiurnal period is explained by the tendency of direction of the main current to the zone of steep depth gradient. Oscillations of currents in the upper layers with diurnal recurrence (September, depths of 0-30 m) could be caused by diurnal changes of meteorological parameters.

Water temperature distributions and internal waves

Water salinity and temperatures data were collected at five stations with use of CTD "Seabird" and MSS sondes. Investigations of salinity near the diffuser show complicated vertical profiles of salinity, which are most probably caused by the intrusion of wastewater discharged from the diffuser. The Aanderaa thermistor chain data enable estimating the temperature variability at station B2 at depths of 18-60 m. Sampled data on the temperature have allowed evaluating the density spectrum of internal gravity-inertial waves in temporal ranges varying from local inertial band ($\omega \approx f$) to short-term intervals of ~15 minutes typical for the Brunt-Väisälä local frequency. Data of analysis clearly shows that there is a strong correlation between the seawater temperature changes registered at the 60-m depth and regular ascending and descending of the oceanic level caused by the tidal forces. It should be noted that the phase of high water (tide) corresponds to an increase of water temperature at depths of 30-60 m. Under these conditions, the thermocline is descending down to deeper levels. Spectral analysis of water temperature shows, that the maximum in spectra is observed at the frequency of semidiurnal oscillations (ω ~ 0,5 rad·h^{-1}) were detected together with several small maxima (the temporal scales varying from 3 to 12 hours). Those spectra reveal the existence of harmonics corresponding to the groups of internal waves having random phases and amplitudes.

The "fast" temperature variations observed above the diffuser, have the major impact on the sewages' surfacing and on the level of pollution concentration in the water area. Sharp changes of temperature and current velocities are possibly related to the internal waves caused by the tidal waves colliding steep coasts. Studies of internal waves were carried out through the analysis of changing isotherm depths. The spectrum of internal waves (see Fig. 1) has the main maximum at

the tidal frequency ($\omega \sim 0.5$ rad·h^{-1}), as well as minor maxima in high frequency range (ω / 1 rad·h^{-1}) caused by short-period internal waves. On the base of data on the depth of 25°C isotherm there was constructed a frequency-temporal spectrum $S(\omega,t)$ built by means of calculating the spectra of internal waves for several time spans belonging to the observation period non stationary spectra of internal waves for different time intervals. These spectra composed for these five time intervals determine the energy distribution at temporal scales varying from diurnal ones to the scales corresponding to the local Brunt-Väisälä frequency $N(z)$. These figures demonstrate essential variability of spectra in time. Generally, the presence of maxima at tidal semidiurnal frequency (ω~0.5 rad·h^{-1}) is observed there. When the energy of semidiurnal tidal waves reaches its maximum, there are no significant maxima in the high frequency (ω/0.5 rad·h^{-1}) spectral range [see Fig. 1 (a)]. When the amplitude of tidal waves decreases in this spectral band, there are observed higher frequency maxima corresponding to 6 and 3 hours. In the high frequency spectral range, there were not detected any important periodic fluctuations, and the slope of the spectrum of internal was proportional to $\omega \sim n^{-2}$ what is typical of internal oceanic waves.

Presence of predominant semidiurnal tidal internal waves with average amplitude of 8 m and diurnal oscillations of considerably smaller amplitudes was also detected. Descending of the thermocline causes intensive internal waves of the lowest mode of 30 m amplitude that could lead to the ascent of discharged sewages to the near-surface level. Spectral analysis of water temperatures time series and temperature fields has allowed us detecting rapid changes of temperature above the diffuser (caused by internal waves, which appear when the tidal waves collide with the steep coast). That leads to the ascending of sewages and to an increase of concentration of pollutants in the water area.

Turbulence and microstructure

Comprehensive measurements of microstructures and turbulence realized by Prof. C. Gibson (Gibson et al., 2003) during the experiment have shown that the discharge jet velocity is a source of strongly active, local turbulence in the immediate diffuser area. Diluted effluent forms a rising, buoyancy driven turbulent plume that is trapped below the sea surface, forming partially fossilized turbulence microstructure patches. The patches are convected by the local currents.

This process of turbulence fossilization and re-generation is repeated along the vertical and stops by wave breaking at the surface, which interferes with the surface wave field. This generates the surface wave field anomalies detected by remote sensing methods. The observed phenomena were caused by other physical mechanisms of interaction at surface and internal waves (Bondur and Grebenuk, 2001).

Surface waves

To determine spectra of surface heaving in the water area of the Mamala Bay, there were used three wave buoys (wave recorders), namely two Directional Waveriders buoys and the Trident Directional Wave buoy. Processing of in-situ measurements enabled to determine parameters describing relevant wave processes observed at those stations and namely, $S(\omega,\theta)$ and $S(\omega)$. An analysis of these spectra $S(\omega)$ observed at the stations was carried out in the spectrum band of $0{,}157 \le \omega \le 3{,}644$ sec^{-1}, i.e. in the band of gravitational waves. They have at least three apparent spectral maximums at the following frequencies: $\omega_{max1} \approx 0{,}41$ s^{-1}, $\omega_{max2} \approx 0{,}69$ s^{-1}, $\omega_{max3} \approx 1{,}57$ s^{-1}. That allows supposing existence of three systems of waves in the water area studied that seriously complicates the analysis of wave processes. Spatial periods of wind driven sea surface heaving could be determined with the help of empirical evaluation of the heaving spectra. For example, use of Pearson-Moskovitz method gives the values of spatial periods varying from 10 m to 55 m. That allows guessing that the wave field observed in the region was affected by two systems of swell waves having average lengths $\lambda \sim 370$ m and $\lambda \sim 130$ m, as well as by the system of

wind driven waves (λ ~ 25 m). Spectral density S(ω) of swell waves of $\lambda^{(1)}_{max}$≈370 m were in 5,8 times greater than that of $\lambda^{(2)}_{max}$≈130 m and about in 22,5 times greater than the value of S(ω) for wind driven waves. Spectral maxima are clearly seen in the frequency-oriented S(ω,θ) spectra enables to determine trends of propagation of selected wage groups and their dynamics.

The values of wave lengths for detected spectral maxima coincide with those derived from "Ikonos-2" imagery spatial spectra $S(k_x,k_y)$ in the range of registered scales.

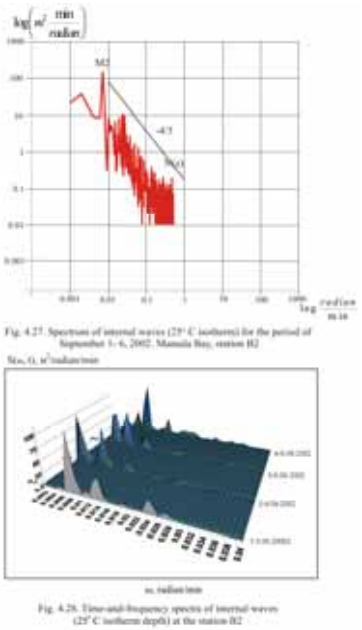

Fig. 1. Spectra of internal waves (calculated from values of the 25°C-isotherm depth)

Summary

The experiment shows main features of oceanographic parameters in the coastal zone. Physical backgrounds for the Detection of Anthropogenic Impact on the Littoral Waters (coastal zone) by remote sensing methods were developed. Various methods, including uncontrollable classification, color-coding, calculation of ratios of band signals and filtration were used for the processing of multi-spectral "Ikonos-2" and ISS imagery taken during the period of our sub-satellite experiments and for the processing of multi-spectral "Ikonos-2" images.

A complex analysis of zones of the sea heaving anomalies highlighted with use of spatial spectra of satellite imagery and the anomalies in the near-surface layers observed in multi-spectral images, and the results of sub-satellite measurements have shown good correlation. Contact measurements of current fields, turbidity, salinity and biological parameters distribution confirm presence of southwest and southeast lobes in zones of anomalies propagation detected at the processing of remotely sensed data. Main harmonics detected in spectra of satellite images were also detected in frequency spectra, measured in the vicinity of the outfall system.

Complex analysis of space data and also hydrophysical and hydrobiological data obtained during *in situ* experiments and spatial spectral processing of "Ikonos-2" images and archival "QuickBird" imagery has allowed us detecting the regions of superficial anomalies caused by deep outfall system of sewage waters, and to determine their shape and size. Some of the anomalous formations studied had a butterfly-shaped form with southwest (214-224^0) extending at about 10 km and having southeast lobes of 6 - 7 km length propagating in the directions of 147-152^0 (see Fig. 2 a). This

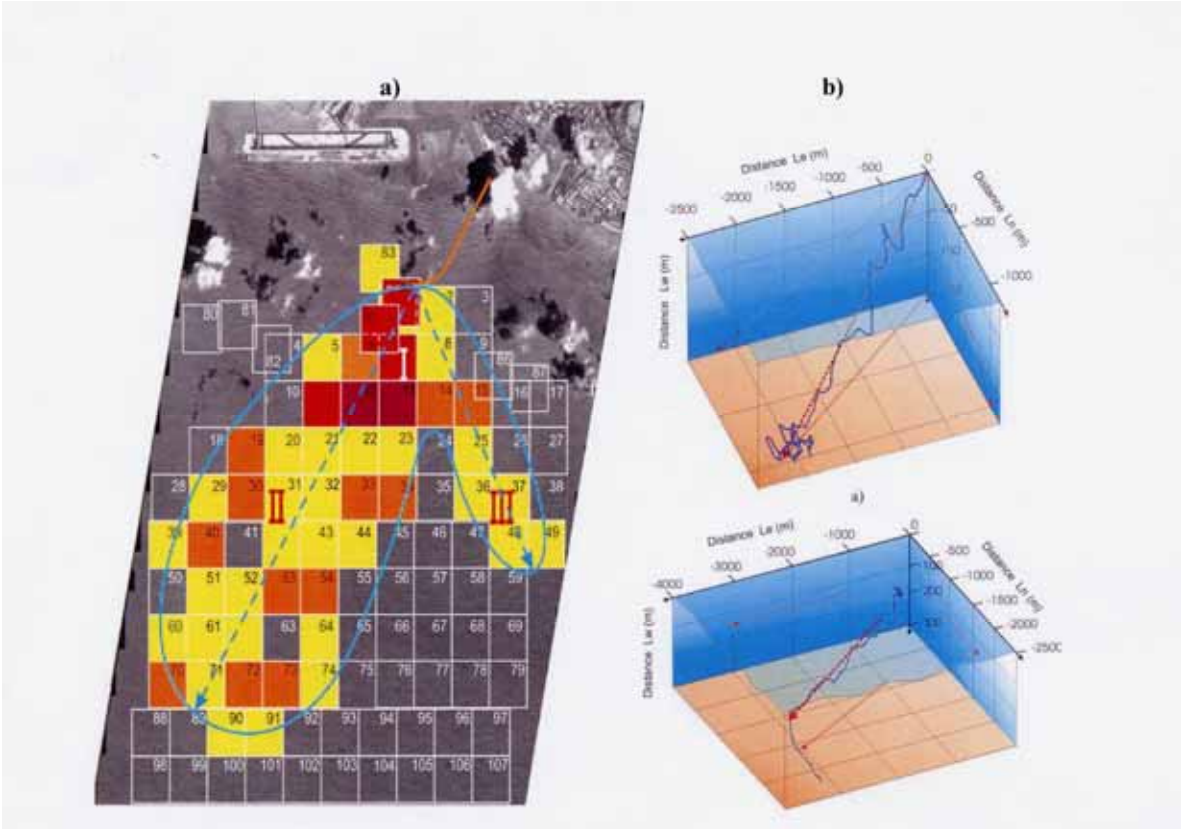

Fig. 2. **a**) Satellite data analysis from IKONOS-2 satellite panchromatic image, 1 m resolution in September 2002. The green boundary line is the outline of the waste field outlining the range of surface wave anomalies. The thick red line is the waste water submerge diffuser pipe coming from the Honolulu is in red at the top of the picture. Intensively of anomaly of manifestation of polluted waters show by colour; **b**) 3-D progressive-vector diagram at the station B2 near diffuser 2.09.02 and 6.09.02.

An analysis of 3D progressive-vector diagrams of currents (Fig. 2 b) are showed well agreement with propagation of superficial manifestations of the deep plume obtained by satellite imagery processing (Fig. 2 a).

Acknowledgements

We are grateful to colleagues from Scientific-educational center "Aerokosmos" and Mr. M. Petrov and Mr. R.Zdorovennov who help us with data analysis.

References

Bondur V.G., Vinogradov M.E., Dolotov U.S., Filatov N.N. at al., 2003. Final Report "Remote Sensing of Anthropogenic Influence caused by submerged sewers on ecosystems of Littoral Waters with use of space methods". Information Systems and Scientific Capacious Technologies, Moscow, 238 p.

Patrick K. Sullivan, Dayananda Vithanage**.** Ocean outfall performance as a function of density gradient variations from internal waves. Hawaii Water Environmental Association 18th Annual Conference, 1996, 11p.

Oceanit. Groundtruthing Measurements Data Report, Honolulu, March 2003, 26 p.

Gibson C. H., P.T. Leung, F. Wolk, and H. Prantke, 2003. Interpretative Report of Microstructure Measurements conducted at the Sand Island Outfall., UCSD, San Diego, March 103 p.p.

Mooers C, 1973. A technique for analysis of pair complex-valued time series. *Deep-Sea Res*., **20**: 1129-1141.

Gonella J., 1972 A rotary-component method for analyzing meteorological and oceanographic vector time series. *Deep-Sea Res.*, **19**: 833-846.

Rozhkov V.A., A.P., Belishev and Yu.P. Klevantcov Ju. P., 1983. *Vector analysis of ocean currents.* L.. 264 p. [In Russian].

Kondratyev K. and N. Filatov (Eds.), 1999. *Limnology and Remote sensing*. Springer-Praxis. London. 412 p.

Bondur, V. and G. Grebenuk, 2001. Remote sensing indications of anthropogenic impacts on sea waters by submerge outfalls: modeling and experiments. *J. Investigations of Earth from Space.* **6**: 49-67.